Contact-style magmatic sulphide mineralisation in the Labrador Trough, northern Québec, Canada: Implications for regional prospectivity

[1*]W.D. Smith, [1]W.D. Maier and [2]I. Bliss

[1]School of Earth and Ocean Sciences, Cardiff University, Cardiff, United Kingdom

[2]Northern Shield Resources, Ottawa, Canada

Corresponding author: smithwd1@cardiff.ac.uk

Abstract

The Labrador Trough in northern Québec is currently the focus of ongoing exploration for magmatic Ni-Cu-PGE sulphide ores. This geological belt hosts voluminous basaltic sills and lavas of the Montagnais Sill Complex, which are locally emplaced amongst sulphidic metasedimentary country rocks. The recently discovered Idefix PGE-Cu prospect represents a stack of gabbroic sills that host stratiform patchy net-textured sulphides (0.2 to 0.4 g/t PGE + Au) over a thickness of ~ 20 m, for up to 7 km. In addition, globular sulphides occur at the base of the sill, adjacent to the metasedimentary floor rocks. Whole-rock and PGE geochemistry indicates that the sills share a common source and that the extracted magma underwent significant fractionation before emplacement in the upper crust. To develop the PGE-enriched ores, sulphide melt saturation was attained before final emplacement, peaking at *R* factors of ~ 10,000. Globular sulphides entrained along the base of the sill ingested crustally-derived arsenic and were ultimately preserved in the advancing chilled margin.

Keywords: Labrador Trough, PGE, magmatic sulphide, mineral exploration

1. Introduction

The Montagnais Sill Complex (MSC) in the Labrador Trough of northern Québec is currently the focus of ongoing exploration for magmatic Ni-Cu-platinum group element (PGE) sulphide deposits. The MSC is considered prospective because it hosts voluminous basaltic rocks (> 10,000 km^2), in proximity to a rifted craton margin (*e.g.,* Begg *et al.* 2010), locally emplaced amongst sulphidic metasedimentary rocks (*e.g.,* Ripley and Li 2013). Despite the apparent prospectivity of the province, exploration remains in its infancy, hindered by a lack in understanding of the ore-forming processes operating in the region. Recent exploration conducted by Northern Shield Resources has identified numerous prospective showings across the Labrador Trough, including the Idefix PGE-Cu prospect.

The Idefix PGE-Cu prospect is located approximately 75 km west of Kuujjuaq (Fig. 1) and encompasses 41 claims over 18.5 km^2. The prospect comprises a sequence of differentiated gabbroic sills, bound by intercalated metapelites of the Baby Formation. To date, 1501 m of diamond drilling across fourteen boreholes has revealed stratiform patchy net-textured sulphide ore, with an average 2PGE (Pt + Pd) grade of 0.2 to 0.4 g/t over a thickness of 16 to 34 m, traceable for approximately 7 km along strike. In this paper, we examine the architecture of the Idefix prospect and investigate the processes that led to its formation.

2. Regional Setting

The Labrador Trough represents a foreland fold-and-thrust belt, extending for ~ 800 km from the Grenville Front to Ungava Bay (Hoffman 1988; Skulski *et al.* 1993). The trough formed during the oblique collision between the Southern Rae Craton and the Superior Craton at 1.84 to 1.82 Ga (Wares and Goutier 1990; Wardle and Van Kranendonk 1996). This collision

instigated pervasive, westward out-of-sequence imbricate thrusting of thick-skinned passive margin sediments, where thrust zones are interpreted to propagate to the base of the crust (Wares and Goutier 1990). Metamorphism increases from west to east, peaking at greenschist facies in the northwest (Perreault and Hynes 1990)

Previous work characterised the stratigraphy of the Labrador Trough using a cyclic system, where cycles 1 and 2 represent episodes of passive margin sedimentation, topped by a third cycle of flysch deposits (Clark and Wares 2005 and references therein). Basalts and subordinate rhyolites were emplaced during cycle 1 at 2169 ± 4 Ma and 2142 ± 4 Ma, respectively, marking the onset of rift-related magmatism (Skulski *et al.* 1993 and references therein). The MSC intruded into sedimentary rocks of cycles 1 and 2 at 1884 ± 1.6 Ma (Findley *et al.* 1995). Co-magmatic basalts of the Willbob and Hellancourt Formations (in the south and north, respectively) were emplaced contemporaneously with the MSC (Rohon *et al.* 1993). Several hypotheses for the tectonomagmatic setting of the MSC have been proposed, including: (1) dextral oblique extension above an east-dipping subduction zone (Hoffman 1990b), (2) dextral transtension along the eastern margin of the Superior Craton, resulting in the formation of pull-apart rift basins (Skulski *et al.* 1993), (3) extension in an ensialic back-arc setting (Corrigan *et al.* 2009), and (4) derivation from a deep-seated mantle plume (Ciborowski *et al*. 2017).

The MSC comprises three major sill types, including (i) aphyric (equigranular) mesogabbros with stratiform gabbroic pegmatites, (ii) glomeroporphyritic and porphyritic gabbros, and (iii) differentiated gabbro sills, sometimes with a basal peridotite cumulate layer. Each of these sill types has been described as hosting magmatic sulphide mineralisation (Clark and Wares 2005). Mineralised sills are concentrated in the upper part of the cycle 2 sedimentary package, which comprises sulphide-bearing sediments of the Baby (in the north)

and Menihek Formations (in the south), suggesting a link between crustal contamination and sulphide melt saturation in the magmas (Clark and Wares 2005).

3. Methods

Grab and channel samples were collected across the Idefix property during field reconnaissance in 2012 and 2013. Additional drill core was acquired from the headquarters of Northern Shield Resources, generated during their 2013 drilling program. Thick and thin sections were petrographically analysed and photomicrographed using a Leica MZ12s microscope with camera attachment at Cardiff University.

In total, sixty whole-rock samples were analysed for lithophile major and trace elements, whereas 706 whole-rock samples were assayed for major lithophile elements, V, Cr, Co, Ni, Cu, Zn, Sr, Pt, Pd, and Au. Twenty-eight whole-rock samples from Idefix property and the surrounding gabbroic rocks were analysed for a full suite of platinum group elements (PGE). All geochemical analyses were performed by ALS Minerals (Vancouver). Sample preparation was completed at ALS Minerals (Timmins) using the PREP-31 package. Lithophile major and trace elements were determined through ICP-AES and ICP-MS respectively, following four-acid digestion of fused beads (ALS codes ME-ICP06, ME-MS81, ME-MS42*, ME-4ACD81, and ME-ICP61a). Loss on ignition (LOI) was determined using the OA-GRA05 package. Sulphur and carbon concentrations were determined using a Leco sulphur analyser, whereby 0.1 g of homogenised sample is combusted at ~ 1350°C and total S and C are measured using a non-dispersive infrared sensor (ALS code ME-IR08). Palladium, Pt, and Au concentrations were determined by ICP-MS, following lead oxide fire assay to produce a precious metal bead (ALS codes FA-FUSPG4 and PGM-MS23). To determine the full suite of six PGE and Au, a precious metal bead was produced via nickel

sulphide fire assay and measured through ICP-MS (ALS codes FA-FUSNS01 and PGM-MS25NS). More information regarding analytical procedures can be found on the ALS Minerals website (www.alsgobal.com). Results for representative samples are presented in Tables 1 and 2. The full dataset, as well as standards and blanks, is reported in Supplementary Material 1.

A Zeiss Sigma HB Field Emission Gun Analytical Scanning Electron Microscope, equipped with two Oxford Instruments 150 mm^2 energy dispersive spectrometers (EDS) was used to generate element maps of the sulphide-bearing rocks. The maps were produced at a working distance of 8.9 mm, an accelerating voltage of 20 kV, and a pixel dwell time of 2000 ms.

4. The Idefix PGE-Cu Prospect

4.1. Historical exploration

Airborne reconnaissance surveys conducted in the 1940s identified numerous gossanous outcrops in the broader area hosting Idefix, which were later identified to be magmatic sulphide showings. In the 1950s, several companies conducted field reconnaissance and geophysical surveys in the vicinity of the Idefix prospect and identified several Ni-Cu showings (Sogemines Development Company 1962; Schilling 1963; De Freneuse 1965). Cities Service Minerals Corporation reported the first PGE values approximately ~ 5 km west of Idefix, in gabbroic rocks grading 10.3 g/t Pd, 3.4 g/t Pt, 11.2% Cu, and < 0.1% Ni (Loring 1975).

La Fosse Platinum Group conducted extensive Ni-Cu-PGE exploration along the eastern half of the Labrador Trough during the 1980s and were the first to identify mineralisation at what is now Idefix (then named Ukunngaalik). Samples of aphyric

mesogabbro returned grades of 5.8 g/t Pd, 2.7 g/t Pt, and 0.8 g/t Au (Avison 1986; La Fosse Platinum Group 1988). The area was not explored further until 2002 when Virginia Mines Incorporated identified additional stratiform sulphide mineralisation with grades of up to 18.1 g/t 2PGE + Au (Savard 2003).

Northern Shield Resources conducted seasonal field surveys across the eastern half of the Labrador Trough from 2011 to 2013. Out of 1,614 samples collected from the region, 934 assayed > 0.1 g/t PGE. The Idefix prospect was staked in 2011 and encompasses 41 claims covering 18.5 km^2. Fourteen diamond-drill holes totalling 1,501 m were drilled along the Idefix ridge (Fig. 1), in which grades of 0.2 to 0.4 g/t 2PGE (Pt and Pd) over 16 to 34 m can be traced intermittently for approximately 7 km.

4.2. Local Geology

The Idefix prospect is located within the Gerido lithotectonic zone defined by Clark and Wares (2005; Fig. 1b). The Gerido zone is characterised by intercalated metasediments, banded iron formations, and volcanic extrusives, intruded by mesogabbroic and ultramafic sills of the MSC. Fine- to medium-grained equigranular mesogabbroic rocks strike NW-SE, with dips varying from 85° to 40° to the east (Fig. 1c).

Borehole 13ID-13 (Fig. 2a) intersects the entire stratigraphy of the Idefix property and has been used to characterise the stratigraphy of the prospect. The country rock consists of stratified metapelites, locally containing subhedral pyrite (Fig. 2b). The contact between the country rock and the composition Idefix sill is sharp and irregular, sometimes characterised by a < 5 cm thermal aureole. The Idefix sill is ~ 100 m thick and has been sub-divided into I1, I2, and I3, based on the presence of sulphide mineralisation, as outlined in detail below.

The Idefix sill is overlain by a further ~ 400-m-thick mesogabbroic hanging wall sill named the Primitive Unit (PU). The PU contains only sparsely disseminated sulphide mineralisation.

Relatively thin stratiform gabbroic pegmatite horizons (< 0.5 m) intermittently occur along the I1-I2 and I3-PU contacts (Fig. 2c-d). The former is typically less defined than the latter, but where present, both contain finely disseminated sulphide mineralisation and bluish, interstitial quartz.

4.3. Petrology of the Idefix and Primitive aphyric gabbro sills

Gabbroic rocks of the Idefix prospect are fine- to medium-grained and composed of partially uralitized anhedral clinopyroxene and partially to completely saussurised subhedral plagioclase (Fig. 3). There is no evidence for serpentinization of olivine in any samples and no discernible deformation. The PU is characterised by a higher relative proportion of clinopyroxene (~ 53 vol.%) at the expense of plagioclase (~ 45 vol.%; Fig. 3a). The Idefix sills generally comprise a higher proportion of modal plagioclase (~ 48 vol.%) than clinopyroxene (~ 46 vol.%; Fig. 3b). Accessory phases (< 2 vol.%) include hornblende, acicular actinolite and tremolite, biotite, anhedral apatite, titanite, and Fe-Ti oxides. Anhedral apatite and clusters of titanite, biotite, Fe-Ti oxide, and rutile are most prevalent in sulphide-bearing samples. The I1 sill differs from the other Idefix sills in that it can locally host up to ~ 3 vol.% interstitial quartz. CIPW normative mineralogy of the gabbroic pegmatites indicates that there is little difference relative to that of the aphyric gabbroic sills. The I3-PU gabbroic pegmatite comprises up to ~ 8 vol.% interstitial quartz, with traces of apatite, biotite, ilmenite, and titanite. The I1-I2 pegmatite is characterised by up to ~ 17 vol.% interstitial quartz (Fig. 3c).

4.4. Nature of mineralisation

Two horizons of mineralisation have been intersected at Idefix: (i) patchy net-textured sulphides (< 5 vol.%; Fig 4a) in the contact zone between I3 and PU, and (ii) globular sulphides (0.5 to 2 cm in diameter) in the basal chilled margin of the Idefix sill (I1; Fig. 4b). Finely disseminated sulphide (< 1 vol.%) is observed throughout the remainder of the Idefix sill (*e.g.,* Giles 2015).

The patchy net-textured ores in the I3-PU contact zone are dominated by pyrrhotite [$Fe_{(1-x)}S$; Po; ~ 60 vol.%], chalcopyrite ($CuFeS_2$; Ccp; ~ 32 vol.%), with subordinate pentlandite [$(Fe,Ni)_9S_8$; Pn; ~ 8 vol.%]. Sparsely disseminated sulphide throughout the remainder of I2 and I3 is generally dominated by Ccp over Po, with little-to-no Pn. Base metal sulphides are spatially associated with apatite (~ 0.2 vol.%) and titanite (~ 0.3 vol.%).

Sulphide globules in I1 are often elliptical and comprise a Po core (~ 62 vol.%), enclosing granular and flame Pn (~ 3 vol.%). Chalcopyrite (~ 33 vol.%) occurs around the exterior of the globules and is disseminated throughout the unit. Chalcopyrite is often spatially associated with sulpharsenides belonging to the cobaltite-gersdorffite series (~ 1 vol.%), sphalerite (< 0.1 vol.%), titanite (< 1 vol.%) and apatite.

5. Results

5.1. Lithophile elements

All gabbroic rocks at Idefix plot within a narrow range of MgO (~ 8 to 14 wt.%; Table 1), in that the PU is generally more primitive (10.4 to 13.9 wt.%) than the Idefix gabbros (8.4 to 12.7 wt.%). Throughout all samples, CaO and Cr/V decrease with decreasing MgO content and FeOt, TiO_2 and Sr increase with decreasing MgO content (Fig. 5a-d). The incompatible element composition of the PU and I3 are generally similar (*e.g.,* TiO_2, K_2O, Sr, and REE),

whereas I2 and I1 show greater enrichment in these elements (Fig. 5e). The greatest spread of data is observed in Cr/V values (Fig. 5d), notably for the PU (Cr/V ~ 2 to 6.5). The average Cr/V content of the Idefix sub-units decreases from I3 (Cr/V 1.9 to 6.3) to I1 (Cr/V 0.8 to 2.9). The majority of samples show a Ni concentration of 200 to 250 ppm. A few samples, notably from I3, show higher Ni (> 300 ppm), despite no variation in MgO content. The high Ni contents correspond to an increase in sulphide content.

Primitive mantle normalised multi-element plots (Fig. 6) show broadly similar profiles for gabbroic rocks. The patterns of the PU and I3 are relatively flat (1 to 2x primitive mantle), with variably negative P anomalies. Sub-units I1 and I2 show slightly enriched patterns (2 to 4x primitive mantle), with less pronounced negative P anomalies and strong positive K anomalies. Local metapelitic rocks of the Baby Formation show strong enrichment in LILEs and LREEs, but a similar HREE level relative to that of the gabbroic units. All gabbroic units are characterised by similar Th/Yb_N (0.4 to 1.1), La/Sm_N (0.8 to 1.2), and Gd/Yb_N (0.8 to 1.2) ratios, whereas metasedimentary units have Th/Yb_N values > 50 and La/Sm_N values > 4.8. Total REE concentration increases with decreasing MgO. All gabbroic units show sub-parallel REE patterns, with weakly positive or negative Eu anomalies (Eu/Eu* ~ 0.8 to 1.2; Table 1).

5.2. *Chalcophile elements*

In all gabbroic samples, chalcophile metal concentrations increase with increasing sulphur (Table 2; Fig. 7a-c). The patchy net-textured ores (I3) are generally more enriched in PGE relative to globular ores (I1; Fig. 7c). This trend may correspond to a difference in the platinum group mineral assemblage of the two ore-bearing horizons. Platinum and Pd show a good positive correlation across both ore-bearing horizons ($R^2 = 0.89$), with an average Pd/Pt

ratio of ~ 2.8 (Fig. 7d). The base metals Cu and Ni show good positive correlations with PGE, with the patchy net-textured ores being relatively more enriched in PGE (Fig. 7e-f).

Nickel, the IPGE (Ir and Ru), and Rh show good positive correlations across all ore-bearing gabbroic rocks (Fig. 8a-c). Regional gabbro (RG) samples represent mineralised mesogabbroic rocks at or near to the Idefix property. All samples have Pd/Ir values between 200 and 500 (Fig. 8d), within the range of basaltic rocks elsewhere (*e.g.*, Maier *et al.* 2008b). Platinum and Au contents broadly increase with increasing Ir (Fig. 8e-f). All ore-bearing rocks at Idefix possess Ni/Ir_N and Cu/Pd_N values < 1 (Fig. 9). All samples (> 0.5 wt.% S) plotted in Figure 9 have been recalculated to 100% sulphide using the method of Barnes and Lightfoot (2005). Both ore types exhibit similar patterns, in that IPGE levels are ~ 100x that of the primitive mantle, whereas PPGE (Rh, Pt, and Pd) levels are 1,000 to 10,000x that of the primitive mantle. Globular ores are more enriched in Au and Cu, relative to patchy net-textured ores. The Idefix profiles are similar to that of the Paladin deposit in the Labrador Trough (see Clark and Wares 2005), which represents PGE-enriched sulphide mineralisation in an aphyric gabbro with stratiform gabbroic pegmatite (deposit type 10d in Clark and Wares, 2005). They also show some similarity to the pattern of the J-M Reef, in that the rocks ores are low in IPGE, high in PPGE, with negative Au anomalies.

Figure 10 shows that the majority of sulphide-bearing gabbroic rocks have Cu/Pd ratios below the range of the primitive mantle. This suggests that the host magma did not lose significant sulphide melt before its final emplacement, which would have resulted in a marked depletion in PGE relative to base metals. Overlain on this plot are *R* factor estimations assuming a parent magma composition similar to high-MgO basalts from the Cape Smith Belt (Barnes *et al.* 1992). Most samples plot between an estimated *R* factor range of 1,000 to 10,000 at < 1 vol.% sulphide, consistent with sulphide volumes observed in rock samples.

5.3. Borehole 13ID-13

The borehole samples the hanging wall PU (15 to 115 m), the Idefix sill (115 to 205 m), and metasedimentary footwall lithologies (205 to 206 m). The latter are marked by a pronounced decrease in MgO, Mg#, and Ni (Fig. 11). The composition of I1 becomes less evolved with height, as reflected by an upward increase in MgO, Mg#, and Cr/V, and a decrease in TiO_2 and Sr. In the contact zone between I1 and I2 is a quartz-bearing intermittent gabbroic pegmatitic horizon, which shows little change in composition with the bounding sub-units. Upward through I2, MgO and Cr/V gradually decrease, whereas S and chalcophile metals (Ni < Cu) increase. From the contact between I2 and I3 upwards, MgO and Cr/V increase toward the PU, whilst TiO_2 and Sr gradually decrease. Similarly, S decreases with height, while chalcophile metals increase, peaking at the contact between I3 and the PU. Mafic and incompatible elements smoothly increase and decrease respectively, into the PU. Chalcophile metal concentrations in the PU are mostly at or close to the detection limit. There is little-to-no variation in Cu/Pd and Pd/Pt values upward through I1 and I2. I3 is characterised by lower Cu/Pd values (< 2,000) and upward decreasing Pd/Pt values. The PU comprises generally higher Cu/Pd values and upward decreasing Pd/Pt values (Fig. 11). These vertical patterns are observed in other drilled boreholes in the property (Supplementary Figure 1).

6. Discussion

6.1. Interpreting the stratigraphic orientation

The orientation of the mafic rocks is of major importance in designing effective ore targeting models. However, trends in whole-rock geochemistry at Idefix are inconclusive. Most differentiation indices (Mg#, Cr/V, Ti, Pd/Ir, and Cu/Pd) show a broad trend towards

relatively unevolved compositions with height across the Idefix sill. While this could suggest that the Idefix sill has been tectonically overturned, it is also known that many mafic intrusions show basal reversals on the scale of meters to hundreds of meters in relation to a progressively decreasing trapped liquid component with height in the sill (*e.g.,* Wingellina Hills; Maier *et al.* 2015).

The Idefix PGE-Cu property belongs to deposit type 10d described by Clark and Wares (2005). Several similarities exist between the Idefix prospect and previously discovered occurrences, including the Paladin, Lac Lafortune, and Lac Larochelle prospects. All of these occurrences reside in the Gerido lithotectonic zone in the northern half of the Labrador Trough and are enriched in PGE relative to base metals. Furthermore, sulphide mineralisation (< 5 vol.%) at these occurrences is confined to stratiform gabbroic pegmatites and the underlying gabbro (Clark and Wares 2005 and references therein). Clark and Wares (2005) state that basal sulphides are not observed in these deposit types and that the stratiform gabbroic pegmatitic horizons represent the roof of the sill. However, globular sulphide is present at the base of the Idefix gabbro (with seemingly no compromise to the Cu/Pd values of the overlying net-textured sulphide) and there is evidence for two stratiform gabbroic pegmatites (*i.e.,* I1-I2 and I3-PU). This could either mean that stratiform gabbroic pegmatites may not be exclusive to the upper portions of the sills or that the Idefix sub-units are all distinct sub-sills.

Most PGE-Cu reefs (*e.g.,* Bushveld Complex, Maier *et al.* 2008 and Penikat, Iljina *et al.* 2015) display a sharp basal peak in PGE concentrations, which is overlain by exponentially decreasing PGE over distances varying from a few decimetres to metres. This is typically interpreted to reflect Rayleigh-type fractionation of PGE in an S-saturated magma (Naldrett *et al.* 2009). However, in few PGE-Cu reefs, PGE contents decrease downward into the footwall rocks (*e.g.,* Merensky Reef, Barnes and Maier 2002; Stillwater Complex, Godel

2007). In the Merensky Reef, this has been ascribed to downward percolation of sulphide liquid into semi-consolidated floor rocks (Barnes and Maier 2002). No obvious systematic change in Cu/Pd and Ni/Cu values preclude the percolation of progressively fractionating sulphide liquid and instead suggests that gravity-driven percolation is responsible for the downward decreasing tails of chalcophile metals observed at Idefix (Mungall and Su 2005).

Sulphide liquid cannot travel for significant distances without dispersing into sub-millimetre disseminations induced by Rayleigh-Taylor instabilities or by dissolving in a depressurising magma (Mavrogenes and O'Neill 1999; Robertson *et al*. 2015). Due to the high density of sulphide melt, it tends to be concentrated along the base of magma bodies. However, globular sulphide documented at Noril'sk-Talnakh are an exception (Arndt *et al*. 2003). These globules are thought to have been transported upward in the host sill by gas bubbles, evidenced by the presence of silicate caps atop sulphide globules (see Barnes *et al.* 2019). Sulphide globules at Idefix do not possess silica caps, nor do they possess a Po-Pn lower margin and a Ccp upper margin, which has been used as geopetal structures for host rocks elsewhere (Prichard *et al.* 2004). However, granular pentlandite between chalcopyrite and pyrrhotite supports *in situ* fractionation for the sulphide globules (*e.g.,* Mansur *et al.* 2019). The occurrence of globules in I1 favours an up-right stratigraphy if this sub-unit represents the base of the Idefix or Primitive sills.

6.2. Sulphide melt saturation

Primitive magmas are typically undersaturated in sulphide melt as they ascend through the crust, due to the inverse relationship between sulphide melt solubility and pressure (*e.g.,* Mavrogenes and O'Neill 1999). As the magma undergoes differentiation, the sulphur content of the melt increases as a result of its incompatibility within silicate minerals. For basaltic

magmas, sulphide melt saturation can be attained either through extensive low-pressure fractional crystallisation (typically 40 to 60%) and/or through assimilation of exogenous sulphur (Mavrogenes and O'Neill 1999; Ripley and Li 2013). In many world-class Ni-Cu-PGE sulphide deposits, the assimilation of sulphur-rich country rock is considered a key process in triggering sulphide segregation (Kabanga, Maier *et al.* 2010; Noril'sk-Talnakh, Ripley *et al.* 2003; Voisey's Bay, Li and Naldrett 1999). However, this process is not necessarily required in the formation of PGE-Cu deposits. Instead, it is argued that in these deposit types, fractional crystallisation drives the magma to sulphide melt saturation, resulting in low volumes of sulphide (~ 1%) and higher *R* factors (> 10,000; Campbell and Naldrett 1979). A third possibility is that the Idefix magmas assimilated and/or entrained proto-ore from antecedent pulses of magma (*i.e.,* PU; Maier 2005; Maier and Groves 2011).

Firstly, there is no evidence that the host magmas at Idefix underwent crustal assimilation (Fig. 12). Binary mixing diagrams between a parent magma with the composition of the co-magmatic Hellancourt basalt (Ciborowski *et al.* 2017) and the local Baby Formation metasediments show that all gabbroic rocks (including the ore-bearing horizons) have assimilated < 5% of the country rock (Fig. 12a-b). This conclusion is consistent with those made for sulphide occurrences in the south of the Labrador Trough (*e.g.,* Chauval *et al.* 1987; Rohon *et al.* 1993). It is also consistent with S/Se ratios that are widely used to constrain the presence of crustal sulphur in magmatic sulphides (Queffurus and Barnes 2015). This is because crustal sulphides typically possess much higher S/Se values than magmatic sulphide. At Idefix, all gabbroic rocks plot either at or below the estimated S/Se mantle range of 2850 to 4300 (Eckstrand and Hulbert 1987). However, country rocks are characterised by low S/Se values (< 2,000). Low S/Se values in the gabbroic rocks are consistent with an interaction between sulphide and S-undersaturated fluids (Queffurus and Barnes 2015). Little-to-no change in La/Sm_N relative to S/Se values

argues against wholesale assimilation of country rock, but can be reconciled with devolatilisation of the pyrite-bearing country rock (*e.g.,* Ripley 1981). Addition of exogenous sulphur and arsenic via country rock devolatilisation to I1 may explain the lower PGE tenors and increased relative proportion of sulpharsenides of the globular ores *(e.g*., Piña *et al.* 2013; Le Vaillant *et al.* 2018) , yet this cannot explain low S/Se values in I3 due to the proximity of this unit to the floor rocks.

For the estimation of the *R* factor, we assume that the parent magma to the Idefix gabbro underwent closed-system fractional crystallisation (Campbell and Naldrett 1979). The Cu concentration is within the Cu range of the co-magmatic Hellancourt basalts of Ciborowski *et al.* (2017; 116 ± 34 ppm). From this, all gabbroic rocks at Idefix plot at approximate *R* factors of 5,000 to 10,000, at a maximum of ~ 1 vol.% sulphide, which is consistent with sulphide proportions observed in drill-core and petrographically.

With no indication of crustal contamination influencing sulphide segregation, one must conclude that the Idefix magma was driven to sulphide melt saturation through differentiation. Clark and Wares (2005) argue that the relationship between disseminated sulphide and gabbroic pegmatites favours a hydrothermal origin. However, Pd/Ir ratios at Idefix are < 500 and there is no prominent negative Pt anomaly (*e.g.,* Barnes and Liu 2012). The Cu/Pd values suggest that no PGE has been lost before the final emplacement of the Idefix magma, yet if sulphide segregated *in situ* after ~ 40 to 60% fractional crystallisation (*i.e.,* Ripley and Li 2013) there would be insufficient PGE-undepleted magma for immiscible sulphide to interact with. It must then be concluded that the Idefix magma became saturated in sulphide melt before its final emplacement (*i.e.,* magma conduit), perhaps aided by the cannibalisation of proto-ore left by antecedent pulses of magma (*e.g.,* Maier, 2005; Maier and Groves 2011).

359

360 ### *6.3. Assessing pre-emplacement fractionation of the Idefix magma*

361 The enrichment in strongly chalcophile metals at Idefix suggests that the parent magma was
362 undepleted in chalcophile metals and was derived from a large degree mantle melt. The flat
363 REE profiles (La/Gd_N = 0.8 to 1.2) of the gabbroic rocks at Idefix are analogous to REE
364 profiles of co-magmatic Hellancourt basalts (Skulski *et al.* 1993; Rohon *et al.* 1993), which,
365 in turn, resemble modern transitional MORB. Olivine (Fo ~ 0.84) is typically the liquidus
366 phase in the Hellancourt basalts (Ciborowski *et al.* 2017). As olivine is not present in the
367 Idefix gabbroic rocks, it is possible that the magmas underwent pre-emplacement fractional
368 crystallisation. Pre-emplacement olivine fractionation would deplete the remaining melt of
369 Ni. However, the gabbroic rocks at Idefix retain Ni values consistent with local basaltic rocks
370 (~ 133 ppm). This is contradicted by the absence of positive Eu anomalies, which is to be
371 expected if the magma had fractionation plagioclase prior to its final emplacement.
372 Moreover, the negative Ru anomalies may be best explained by pre-emplacement
373 fractionation of spinel (Righter *et al.* 2004; Pagé and Barnes 2012). It is therefore, possible
374 that the magma parental to the Idefix sills and associated basaltic rocks underwent pre-
375 emplacement fractionation in the lower crust (*e.g.,* Skulski *et al.* 1993; Heinonen *et al.* 2019).

376

377 ### *6.4. Emplacement and orientation of the gabbroic rocks at Idefix*

378 From the current data, it remains unclear if the strata at Idefix has been tectonically
379 overturned or not (see Fig. 13). The presence of two distinct sulphide-bearing horizons
380 suggests at least two episodes of sill emplacement has occurred at Idefix, yet the sequence of
381 emplacement is difficult to discern:

382 Scenario 1: *Sequentially emplaced and overturned*:

In this scenario, the PU was first emplaced, followed by I3 + I2, and then I1. To constrain the way-up of the PU, the eastern contact of this unit must be characterised. From the current data, there is no evidence that the PU overlying the Idefix sill is the upper part of a differentiating sill (MgO > 10 wt.%, TiO_2 < 0.5 wt.%). Although, it remains possible that this could represent a reversal if emplaced against the country rock. The Idefix sill was emplaced, whilst entraining immiscible sulphide, which underwent gravity-driven percolation to begin to accumulate on the I3-PU contact (Mungall and Su 2005). Lastly, I1 was emplaced entraining immiscible sulphide globules. However, if emplaced last, antecedent pulses of magma would have already devolatilised the country rock, precluding the formation of sulpharsenides by ingestion of crustally derived As. In this model, the gabbroic pegmatites form via static recrystallisation as described by Barnes and Maier (2002). The sequence was then tectonically overturned during the waning stages of the New Québec Orogeny. However, current mapping data support a regionally NE-facing sequence (M. Houlé, written communication, 2019),

Scenario 2: *Non-sequentially emplaced and overturned*:

In this scenario, PU and I1 were emplaced before I2 + I3, whereby I1 represents the upper chilled margin of the PU. This is consistent with the generally chalcophile-depleted character of the PU (Cu/Pd ≥ 10,000, PGE < 0.1 ppm). The density of sulphide melt typically precludes their occurrence in the upper parts of host sills, yet this has been documented elsewhere (*i.e.,* Noril'sk-Talnakh) due to volatile-rich bubbles (Barnes *et al.* 2019). However, the absence of silica caps around the globules, together with the high settling velocities of sulphide liquid (Chung and Mungall 2009) makes this unlikely at Idefix. The Idefix magmas were then emplaced below the advancing chilled margin, where entrained sulphide percolated to the

base of the sill. The I3-PU gabbroic pegmatite would have formed via static recrystallisation, yet the formation of the I1-I2 pegmatite may have been influenced by magmatic fluids exsolved from the Idefix magma. However, the current data cannot support this hypothesis.

Scenario 3: *Sequentially emplaced*:

In this scenario, each sill represents an individual pulse of magma. Firstly, I1 was emplaced entrained immiscible sulphide globules that ingested crustally derived S and As. Secondly, I2 was emplaced, forming a discontinuous gabbroic pegmatite via static recrystallisation. Thirdly, I3 was emplaced, whilst entraining PGE-rich immiscible sulphide. A gabbroic pegmatite has not been identified between I2 and I3, meaning that these units could represent one pulse of magma. Lastly, the PU was emplaced above the Idefix sill. The I3-PU gabbroic pegmatite is better preserved than the one present at the I1-I2 contact since the PU is thicker and less evolved than the Idefix sill.

Scenario 4: *Non-sequentially emplaced*:

In this scenario, PU and I1 were emplaced before the Idefix sills, similar to that described in Scenario 2. This model can be reconciled with the (i) low PGE concentrations of the overlying PU and (ii) the assimilation of exogenous S and As from the country rock floor. The Idefix sill was progressively emplaced above the advancing chilled margin of the PU (*i.e.,* I1). The I2 and I3 units may have been emplaced as two separate pulses, in that the I3 unit entrained a higher volume of immiscible sulphide as evidenced in the drill-core geochemistry (Fig. 11; Supplementary Figure 1).

6.5. Potential for PGE-Cu deposits in the Labrador Trough

In the Labrador Trough, PGE-Cu deposits are exclusive to aphyric gabbro sills in the Gerido lithotectonic zone (*e.g.,* Paladin, Lac Lafortune, and Lac Larochelle; Clark and Wares 2005). Their enrichment in PGE (Cu/Pd < 10,000) indicates that the parental magmas were undersaturated in sulphide melt during their emplacement. This suggests that they could have produced economic contact-style mineralisation. This deposit type is not necessarily dependent on the assimilation of crustal sulphur. Country rock in proximity to the Idefix sill is only locally sulphide-bearing and the Idefix sill (< 100 m) would not possess the heat required to effectively assimilate the country rocks. Although sulphidic country rock is not necessarily required for this deposit type, it remains a prospective characteristic if the intrusive sill is able to effectively extract crustal sulphide. The presence of stratiform pegmatitic gabbro with disseminated sulphide can be considered a good indicator of proximity to PGE-rich sulphide mineralisation in aphyric gabbro sills of the Montagnais Sill Complex. It is favourable that sills with stratiform gabbroic pegmatite are thick (> 100 m) and bound by other mafic-ultramafic sills, so that slower cooling rates may allow for pronged interaction between silicate melt and sulphide liquid.

7. Conclusions

The Idefix PGE-Cu prospect in the Labrador Trough, northern Québec represents a stack of differentiated gabbroic sills (~ 8 to 14 wt.% MgO, ~ 1 to 8 Cr/V), which are host to stratiform patchy net-textured and globular sulphide horizons, associated with stratiform gabbroic pegmatites. Primary minerals of the gabbroic hosts have undergone moderate to extensive alteration, whereby pyroxene is partially to completely replaced by amphibole, and plagioclase is almost completely saussurised. The patchy net-textured ores are more enriched

in chalcophile metals relative to the globular ores. Chalcophile metals in each horizon generally show good positive inter-element correlations (Ni/Cu = 0. 85; Cu/Pd = 0.68, Pd/Pt = 0.92, and IPGE/Ru = 0.96). Low Ni and IPGE tenors are ascribed to pre-emplacement fractionation of olivine and spinel. There is no evidence for the assimilation of crustal rock ($La/Sm_N \leq 1$ and $Th/Yb_N \leq 1$) or addition of exogenous sulphur ($S/Se \leq 4{,}00$). Furthermore, *in situ* segregation of sulphide melt is precluded by insufficient volumes of PGE-undepleted magma to generate the observed PGE-Cu mineralisation. Henceforth, immiscible sulphide melt segregated before its final emplacement and was entrained upward. The patchy net-textured ores formed at *R* factors of up to 10,000, which was assisted by prolonged cooling rates due to thermal priming by antecedent pulses of magma. However, sills must be sufficiently thick (> 100 m) and bound by hot mafic-ultramafic rocks to slow the cooling rate of the host sill. This allows for sulphide to interact with a greater volume of silicate magma and gives time to settle into narrow, PGE-rich reef-style horizons.

Funding

W.D. Smith acknowledges the NERC GW4$^+$ doctoral training partnership (NE/L002434/1) for funding analytical procedures. Northern Shield Resources are thanked as acting as CASE partner for the project.

Acknowledgements

The authors thank colleagues at Northern Shield Resources for fieldwork assistance, sampling, and data processing, as well as allowing publication of the data. Nick Giles is acknowledged for undertaking optical and electron microscopy of Idefix samples. Antony Oldroyd and Duncan Muir are all thanked for assistance and guidance during data

478 acquisition. This paper was greatly improved by thorough reviews from E. Mansur and C.M.
479 Lesher and additional comments from T.G. Blenkinsop. We thank Ali Polat for the editorial
480 handling of this manuscript.

481

482 **References**

483 Arndt, N. T., Czamanske, G. K., Walker, R. J., Chauvel, C., and Fedorenko, V. A. (2003).
484 Geochemistry and origin of the intrusive hosts of the Noril'sk-Talnakh Cu-Ni-PGE sulfide
485 deposits. Economic Geology, 98: 495-515.

486 Avison, A. T. (1986). Report on 1986 Exploration Program in the Labrador Trough.
487 Geological Association of Canada.

488 Barnes, S-J., and Lightfoot, P.C. (2005). Formation of magmatic nickel-sulfide ore deposits
489 and processes affecting their copper and platinum-group element contents. In Hedenquist,
490 J.W., Thompson, J.F.H., Goldfarb, R.J. and Richards, J.P. Economic Geology 100: 179-213.

491 Barnes, S.-J., and Maier, W. D. (1999). The fractionation of Ni, Cu and the noble metals in
492 silicate and sulfide liquids. Geological Association of Canada, 13: 69–106.

493 Barnes, S.-J., Picard, C., Giovenazzo, D., and Tremblay, C. (1992). The composition of
494 nickel-copper sulphide deposits and their host rocks from the Cape Smith Fold Belt, Northern
495 Quebec. Australian Journal of Earth Sciences, 39(3), 335-347.

496 Barnes, S. J., and Maier, W. D. (2002). Platinum-group elements and microstructures of
497 normal Merensky reef from Impala Platinum Mines, Bushveld Complex. Journal of
498 Petrology, 43(1), 103-128.

499 Barnes, S. J., & Liu, W. (2012). Pt and Pd mobility in hydrothermal fluids: evidence from
500 komatiites and from thermodynamic modelling. Ore Geology Reviews, 44, 49-58.

501 Barnes, S.J., Mungall, J.E., Le Vaillant, M., Godel, B., Lesher, C.M., Holwell, D., Lightfoot,
502 P.C., Krivolutskaya, N. and Wei, B. (2017). Sulfide-silicate textures in magmatic Ni-Cu-PGE
503 sulfide ore deposits: Disseminated and net-textured ores. American Mineralogist, 102: 473-
504 506.

505 Barnes, S. J., Le Vaillant, M., Godel, B., and Lesher, C. M. (2018). Droplets and Bubbles:
506 Solidification of Sulphide-rich Vapour-saturated Orthocumulates in the Norilsk-Talnakh Ni–
507 Cu–PGE Ore-bearing Intrusions. Journal of Petrology, 60(2), 269-300.

508 Begg, G. C., Hronsky, J. A., Arndt, N. T., Griffin, W. L., O'Reilly, S. Y., and Hayward, N.
509 (2010). Lithospheric, cratonic, and geodynamic setting of Ni-Cu-PGE sulfide
510 deposits. Economic geology, 105: 1057-1070.

511 Campbell, I. H., and Naldrett, A. J. (1979). The influence of silicate: sulfide ratios on the
512 geochemistry of magmatic sulfides. Economic Geology, 74(6), 1503-1506.

513 Chauvel, C., Arndt, N. T., Kielinzcuk, S., and Thom, A. (1987). Formation of Canadian 1.9
514 Ga old continental crust. I: Nd isotopic data. Canadian Journal of Earth Sciences, 24: 396–
515 406.

516 Chung, H. Y., and Mungall, J. E. (2009). Physical constraints on the migration of immiscible
517 fluids through partially molten silicates, with special reference to magmatic sulfide
518 ores. Earth and Planetary Science Letters, 286(1-2), 14-22.

519 Ciborowski, T. J. R., Minifie, M. J., Kerr, A. C., Ernst, R. E., Baragar, B., and Millar, I. L.
520 (2017). A mantle plume origin for the Palaeoproterozoic Circum-Superior large Igneous
521 Province. Precambrian Research, 294: 189-213.

522 Clark, T., and Wares, R. (2005). Lithotectonic and Metallogenic Synthesis of the New
523 Quebec Orogen (Labrador Trough).

524 Corrigan, D., Pehrsson, S., Wodicka, N., and de Kemp, E. (2009). The Palaeoproterozoic
525 Trans-Hudson Orogen: a prototype of modern accretionary processes. Geological Society,
526 London, Special Publications, 327: 457–479.

527 De Freneuse, S. W. (1965). A Report on the Gravity Survey.Eckstrand, O. R., and Hulbert, L.
528 J. (1987). Selenium and the source of sulfur in magmatic nickel and platinum deposits [abs.].
529 In Geological Association of Canada-Mineralogical Association Canada Program with
530 Abstracts (Vol. 12, p. 40).

531 Eckstrand, O. R., & Hulbert, L. J. (1987). Selenium and the source of sulfur in magmatic
532 nickel and platinum deposits [abs.]. In Geological Association of Canada-Mineralogical
533 Association Canada Program with Abstracts (Vol. 12, p. 40).

534 Findlay, J. M., Parrish, R. R., Birkett, T. C., and Watanabe, D. H. (1995). U-Pb ages from the
535 Nimish Formation and Montagnais glomeroporphyritic gabbro of the central New Quebec
536 Orogen, Canada, 1220: 1208–1220.

537 Giles, N.K. (2015). The Timing and Control of PGE-Bearing Sulphide Droplet Dispersal in a
538 Silicate Dominated System at the Idefix Property, Northern Québec, Canada. MSc Thesis.

539 Godel, B. (2007). Rôle des liquides sulfures dans la formation des mineralisations riches en
540 elements du groupe du platine: applications au complexe du bushveld (afrique du sud) et au
541 complexe de stillwater (états-unis). PhD Thesis.

542 Heinonen, J. S., Luttinen, A. V., Spera, F. J., & Bohrson, W. A. (2019). Deep open storage
543 and shallow closed transport system for a continental flood basalt sequence revealed with
544 Magma Chamber Simulator. Contributions to Mineralogy and Petrology, 174(11), 87.

Hinchey, J. G., Hattori, K. H., and Lavigne, M. J. (2005). Geology, petrology, and controls on PGE mineralization of the southern Roby and Twilight zones, Lac des Iles mine, Canada. Economic Geology, 100(1), 43-61.

Hoffman, P. F. (1988). United plates of America, the birth of a craton: Early Proterozoic assembly and growth of Laurentia. Annual Review of Earth and Planetary Sciences, 16(1), 543-603.

Hoffman, P. F. (1990). Dynamics of the tectonic assembly of Northeast Laurentia in geon 18 (1.9-1.8 Ga). Geoscience Canada, 17.

Iljina, M., Maier, W. D., and Karinen, T. (2015). PGE-(Cu-Ni) deposits of the Tornio-Näränkävaara belt of intrusions (Portimo, Penikat, and Koillismaa). In Mineral deposits of Finland (pp. 133-164).

La Fosse Platinum Group. (1988). Report on 1987 Exploration Results on Permits 809, 810, 811 Lac De Freneuse District.

Le Vaillant, M., Barnes, S. J., Fiorentini, M. L., Barnes, S. J., Bath, A., and Miller, J. (2018). Platinum-group element and gold contents of arsenide and sulfarsenide minerals associated with Ni and Au deposits in Archean greenstone belts. Mineralogical Magazine, 82(3), 625-647.

Li, C., and Naldrett, A. J. (1999). Geology and petrology of the Voisey's Bay intrusion: reaction of olivine with sulfide and silicate liquids. Lithos, 47(1-2), 1-31.

Loring, W. B. (1975). Report on the Big “M” Property, Labrador Trough. Ministere Des Richesses Naturelles.

566 Maier, W. D. (2005). Platinum-group element (PGE) deposits and occurrences:
567 Mineralization styles, genetic concepts, and exploration criteria. Journal of African Earth
568 Sciences, 41(3), 165-191.

569 Maier, W. D., De Klerk, L., Blaine, J., Manyeruke, T., Barnes, S. J., Stevens, M. V. A., and
570 Mavrogenes, J. A. (2008a). Petrogenesis of contact-style PGE mineralization in the northern
571 lobe of the Bushveld Complex: comparison of data from the farms Rooipoort, Townlands,
572 Drenthe and Nonnenwerth. Mineralium Deposita, 43(3), 255-280.

573 Maier, W. D., Barnes, S. J., Chinyepi, G., Barton, J. M., Eglington, B., and Setshedi, I.
574 (2008b). The composition of magmatic Ni–Cu–(PGE) sulfide deposits in the Tati and Selebi-
575 Phikwe belts of eastern Botswana. Mineralium Deposita, 43(1), 37-60.

576 Maier, W. D., Barnes, S. J., Sarkar, A., Ripley, E., Li, C., and Livesey, T. (2010). The
577 Kabanga Ni sulfide deposit, Tanzania: I. Geology, petrography, silicate rock geochemistry,
578 and sulfur and oxygen isotopes. Mineralium Deposita, 45(5), 419-441.

579 Maier, W. D., & Groves, D. I. (2011). Temporal and spatial controls on the formation of
580 magmatic PGE and Ni–Cu deposits. Mineralium Deposita, 46(8), 841-857.

581 Maier, W.D., Howard, H.M., Smithies, R.H., Yang, S.H., Barnes, S.-J., O'Brien, H., Hannu,
582 H. and Gardoll, S. (2015). Magmatic ore deposits in mafic–ultramafic intrusions of the Giles
583 Event, Western Australia. Ore Geology Reviews, 71: 405-436.

584 Mansur, E. T., Barnes, S. J., & Duran, C. J. (2019). Textural and compositional evidence for
585 the formation of pentlandite via peritectic reaction: Implications for the distribution of highly
586 siderophile elements. Geology, 47(4), 351-354.

587 Mavrogenes, J. A., and O'Neill, H. S. C. (1999). The relative effects of pressure, temperature
588 and oxygen fugacity on the solubility of sulfide in mafic magmas. Geochimica et
589 Cosmochimica Acta, 67: 1173-1180.

590 Mungall, J. E., & Su, S. (2005). Interfacial tension between magmatic sulfide and silicate
591 liquids: Constraints on kinetics of sulfide liquation and sulfide migration through silicate
592 rocks. Earth and Planetary Science Letters, 234(1-2), 135-149.

593 Mungall, J. E., and Brenan, J. M. (2014). Partitioning of platinum-group elements and Au
594 between sulfide liquid and basalt and the origins of mantle-crust fractionation of the
595 chalcophile elements. Geochimica et Cosmochimica Acta, 12: 265-289.

596 Naldrett, A. J., Wilson, A., Kinnaird, J., and Chunnett, G. (2009). PGE tenor and metal ratios
597 within and below the Merensky Reef, Bushveld Complex: implications for its
598 genesis. Journal of Petrology, 50: 625-659.

599 Pagé, P., Barnes, S. J., Bédard, J. H., and Zientek, M. L. (2012). In situ determination of Os,
600 Ir, and Ru in chromites formed from komatiite, tholeiite and boninite magmas: implications
601 for chromite control of Os, Ir and Ru during partial melting and crystal
602 fractionation. Chemical Geology, 302, 3-15.

603 Perreault, S., and Hynes, A. (1990). Tectonic evolution of the Kuujjuaq terrane, New Québec
604 Orogen. Geoscience Canada, 17: 238–240.

605 Piña, R., Gervilla, F., Barnes, S. J., Ortega, L., and Lunar, R. (2013). Partition coefficients of
606 platinum group and chalcophile elements between arsenide and sulfide phases as determined
607 in the Beni Bousera Cr-Ni mineralization (North Morocco). Economic Geology, 108(5), 935-
608 951.

609 Prichard, H. M., Hutchinson, D., and Fisher, P. C. (2004). Petrology and crystallization
610 history of multiphase sulfide droplets in a mafic dike from Uruguay: implications for the
611 origin of Cu-Ni-PGE sulfide deposits. Economic Geology, 99(2), 365-376.

612 Queffurus, M., and Barnes, S. J. (2015). A review of sulfur to selenium ratios in magmatic
613 nickel–copper and platinum-group element deposits. Ore Geology Reviews, 69, 301-324.

614 Righter, K., Campbell, A. J., Humayun, M., and Hervig, R. L. (2004). Partitioning of Ru, Rh,
615 Pd, Re, Ir, and Au between Cr-bearing spinel, olivine, pyroxene and silicate
616 melts. Geochimica et Cosmochimica Acta, 68(4), 867-880.

617 Ripley, E. M. (1981). Sulfur isotopic studies of the Dunka Road Cu-Ni deposit, Duluth
618 Complex, Minnesota. Economic Geology, 76(3), 610-620.

619 Ripley, E. M., Lightfoot, P. C., Li, C., and Elswick, E. R. (2003). Sulfur isotopic studies of
620 continental flood basalts in the Noril'sk region: Implications for the association between
621 lavas and ore-bearing intrusions. Geochimica et Cosmochimica Acta, 67(15), 2805-2817.

622 Ripley, E. M., and Li, C. (2013). Sulfide saturation in mafic magmas: Is external sulfur
623 required for magmatic Ni-Cu-(PGE) ore genesis?. Economic Geology, 108(1), 45-58.

624 Robertson, J. C., Barnes, S. J., and Le Vaillant, M. (2015). Dynamics of Magmatic Sulphide
625 Droplets during Transport in Silicate Melts and Implications for Magmatic Sulphide Ore
626 Formation. Journal of Petrology, 56: 2445–2472.

627 Rohon, M.-L., Vialette, Y., Clark, T., Roger, G., Ohnenstetter, D., and Vidal, P. (1993).
628 Aphebian mafic - ultramafic magmatism in the Labrador Trough (New Quebec): its age and
629 the nature of its mantle source. Canadian Journal of Earth Sciences, 30: 1582-1593.

630 Savard, M. (2003). Labrador Trough Project: Summer 2002 Technical Report.

631 Schilling, J.-G. (1963). Report on West Anderson Lake Group.

632 Seat, Z., Beresford, S. W., Grguric, B. A., Waugh, R. S., Hronsky, J. M., Gee, M. M.,
633 Groves, D. I. and Mathison, C. I. (2007). Architecture and emplacement of the Nebo–Babel
634 gabbronorite-hosted magmatic Ni–Cu–PGE sulphide deposit, West Musgrave, Western
635 Australia. Mineralium Deposita, 42(6), 551.

636 Skulski, T., Wares, R. P., and Smith, A. D. (1993). Early Proterozoic (1.88-1.87 Ga) tholeiitic
637 magmatism in the New Quebec orogen. Canadian Journal of Earth Sciences, 30: 1505–1520.

638 Sun, S. S., and McDonough, W. F. (1989). Chemical and isotopic systematics of oceanic
639 basalts: implications for mantle composition and processes. Geological Society, London,
640 Special Publications, 42(1), 313-345.

641 Sogemines Development Company. (1962). Ungava Gossans Project Geological Report.

642 Wardle, R. J., and Kranendonk, M. J. Van. (1996). The Palaeoproterozoic Southeastern
643 Churchill Province of Labrador-Quebec, Canada: orogenic development as a consequence of
644 oblique collision and indentation. Precambrian Crustal Evolution in the North Atlantic
645 Region, 112: 137–153.

646 Wares, R. P., and Goutier, J. (1990). Deformational style in the foreland of the northern New
647 Québec Orogen. Geoscience Canada, 17.

Figure Captions

Figure 1. a. Location of the study area in the lithotectonic divisions of Clark and Wares (2005). b. Geological map of the Idefix PGE-Cu prospect, showing the outline of the property and location of the boreholes addressed in this study. c. Cross-section across the centre of the property, showing the intersections of the labelled boreholes.

Figure 2. a. Schematic stratigraphy of the Idefix PGE-Cu prospect, showing the divisions of the Idefix sill. b. Textures and characteristics of the Baby Formation metasediments. c. Nature of the gabbroic pegmatite at the I1-I2 contact. d. Nature of the gabbroic pegmatite at the I3-PU contact. rill core is ~ 4 cm in diameter. BF = Baby Formation, py = pyrite, qtz = quartz.

Figure 3. Texture and petrography of (a) the Primitive Unit. (b) Idefix unit I3 and I2, (c) Idefix unit I1. d. CIPW normative mineralogy of gabbroic and gabbroic pegmatitic rocks at Idefix. cpx = clinopyroxene, plg = plagioclase, amp = amphibole, qtz = quartz.

Figure 4. a. Texture and mineralogy of patchy net-textured sulphide. b. Texture and mineralogy of globular sulphide. Note the elliptical shape of the sulphide globules. po = pyrrhotite, pn = pentlandite, ccp = chalcopyrite, ars = sulpharsenides.

Figure 5. a-f. MgO against CaO, FeOt, TiO_2, Cr/V, Sr, and Ni.

Figure 6. a-b. Primitive mantle normalised (Sun and McDonough 1989) lithophile multi-element plots.

Figure 7. a-c. Sulphur against Ni, Cu, and 2PGE + Au. d. Pd against Pt, whereby net-textured and globular ores correlate at Pt/Pd values of ~ 2.8. e. Cu against 2PGE + Au. f. Ni against 2PGE + Au. Note the different trends in net-textured and globular ores in plots c, e, and f.

Figure 8. a-f. Ir against Ni, Ru, Rh, Pd, Pt, and Au. Note that IPGE and Pt show good positive correlations ($R^2 > 0.8$) and that all samples plot with Pd/Ir values below 500. RG = regional gabbro.

Figure 9. Primitive mantle normalised (Barnes and Maier 1999) chalcophile multi-element plots for (a) patchy net-textured ores and (b) globular ores. For comparison, profiles form the J-M Reef (Godel *et al.* 2002), Roby Zone of Lac des Iles (LDI; Hinchey *et al.* 2005), Merensky Reef (Barnes and Maier 2002), the Platreef at Rooipoort (Maier *et al.* 2008a), and the Paladin deposit in the Labrador Trough (Clark and Wares 2005). All samples with > 0.5 wt.% S have been normalised to 100% sulphide using the method of Barnes and Lightfoot (2005).

Figure 10. Pd against Cu/Pd with marginal histograms. The underlain grey field represents the expected Cu/Pd range of mantle rock (Barnes and Maier 1999). Grey boxes represent the composition of sulphide at different whole-rock volumes at different *R* factors (see text for discussion).

Figure 11. Downhole geochemistry of borehole 13ID-13, showing the downward trend of lithophile and chalcophile elements.

Figure 12. a-b. La/Sm_N against La/Yb_N and La/Nb_N against Th/Yb_N, overlain with binary mixing models between Hellancourt basalt (Ciborowski *et al.* 2017) and Baby Formation sediments. c. S against Se underlain with that of mantle range (2850 to 4300; Eckstrand and Hulbert 1987). Note that all samples plot at or just below that expected for mantle rock. d. S/Se against La/Sm_{CN} showing no changes in La/Sm_N values relative to S/Se. Normalised ratios were normalised using values of Sun and McDonough (1989).

Figure 13. Emplacement scenarios for the gabbroic rocks at Idefix if (1) sequentially emplaced and overturned, (2) non-sequentially emplaced and overturned, (3) sequentially emplaced, and (4) non-sequentially emplaced.

Table 1. Representative whole-rock compositions of the rocks at Idefix. Full data reported in Supplementary data 2.

Rock Type	PU	PU	Transitional	I3	I3	I2	I2	I1	I1	Sediments
Hole ID	13ID-13	13ID-13	13ID-04	13ID-13	13ID-02	13ID-02	13ID-04	13ID-13	13ID-02	13ID-07
Depth (m)	15.2	62	18.6	116.6	41	88.8	69.7	191.7	118.6	81
Major Elements (wt.%)										
SiO_2	49.5	49.3	49.6	48.5	48.5	48.4	48.2	48.6	48.5	59.8
TiO_2	0.3	0.3	0.4	0.4	0.4	0.5	0.5	0.5	0.6	0.4
Al_2O_3	11.5	13.1	13.7	13.1	13.6	14.6	14.6	13.6	14.0	14.2
Fe_2O_3	7.2	7.7	8.0	8.5	8.9	9.5	9.6	9.5	10.7	11.6
MnO	0.2	0.2	0.2	0.2	0.2	0.2	0.2	0.2	0.2	0.2
MgO	11.6	11.2	10.7	10.9	11.1	10.0	10.2	9.6	9.7	2.9
CaO	16.1	14.5	15.0	13.8	13.9	12.9	13.3	13.5	12.3	2.7
Na_2O	0.6	0.9	1.1	1.1	1.1	1.2	1.3	1.1	1.1	2.6
K_2O	0.0	0.0	0.1	0.1	0.1	0.1	0.1	0.1	0.4	3.8
P_2O_5	0.0	0.0	0.0	0.0	0.0	0.0	0.0	0.0	0.0	0.1
LOI	2.1	2.2	2.2	2.3	2.3	2.6	2.7	2.1	0.5	1.2
Total	99.3	99.6	100.9	98.9	100.0	100.0	100.6	98.9	98.0	99.6
Trace Elements (ppm)										
S (wt.%)	0.0	0.0	0.0	0.1	0.1	0.1	0.1	0.1	0.4	0.1
Sc	52	44	45	42	42	36	36	38	32	9
V	194	195	204	181	199	214	210	229	226	53
Cr	1890	1400	1390	1120	1250	800	840	880	710	50
Co	38	42	37	46	48	47	42	47	54	11
Ni	171	159	137	261	256	179	175	171	331	22
Cu	61	58	55	484	381	195	128	207	710	5
Zn	50	43	43	56	52	58	59	62	67	111
As	1.8	0.6	0.7	0.6	1.1	8.5	1.6	19.0	41.1	0.5
Rb	0.2	1.0	0.8	1.2	1.7	3.7	1.4	1.4	11.6	162.0
Sr	54	65	74	62	66	74	73	84	83	219
Y	7.6	7.9	9.6	8.5	9.1	10.4	10.3	11.7	11.5	14.8
Zr	7	10	17	13	17	21	22	28	29	174
Nb	0.6	0.7	0.7	0.8	0.8	1.0	1.1	1.4	1.3	7.6
Sb	0.1	0.1	0.1	0.2	0.1	0.2	0.3	0.2	0.2	0.1
Cs	<0.01	0.0	0.0	0.0	0.1	0.1	0.0	0.0	0.1	7.6
Ba	5	10	10	12	15	22	10	10	48	426
Th	0.1	0.1	0.2	0.1	0.1	0.2	0.2	0.2	0.2	13.5
Precious Metals (ppm)										
Pd	bdl	0.02	0.01	0.25	0.21	0.06	0.05	0.06	0.17	bdl
Pt	bdl	0.02	0.01	0.09	0.07	0.03	0.02	0.02	0.05	bdl
Au	bdl	bdl	bdl	0.02	0.02	bdl	bdl	bdl	0.01	bdl
REEs (ppm)										
La	1.3	0.9	2.4	1.0	1.2	1.5	1.5	1.7	1.7	43.9
Ce	2.0	2.3	4.4	2.7	3.2	3.9	3.8	4.0	4.6	79.1
Pr	0.3	0.4	0.6	0.5	0.5	0.7	0.6	0.7	0.7	8.6
Nd	1.8	2.0	3.0	2.4	2.7	3.0	3.0	3.9	3.6	30.5
Sm	0.6	0.8	0.9	0.9	0.8	1.1	1.1	1.2	1.3	4.8

Eu	0.3	0.3	0.4	0.4	0.4	0.4	0.5	0.5	0.5	1.0
Gd	1.0	1.1	1.5	1.4	1.4	1.6	1.7	1.8	1.6	3.9
Tb	0.2	0.2	0.2	0.2	0.2	0.2	0.3	0.3	0.3	0.5
Dy	1.5	1.4	1.6	1.5	1.6	1.7	1.8	1.9	2.0	3.0
Ho	0.3	0.3	0.3	0.4	0.3	0.4	0.4	0.5	0.4	0.6
Er	0.8	0.8	1.1	1.0	1.1	1.1	1.1	1.4	1.2	1.7
Tm	0.1	0.1	0.1	0.2	0.1	0.1	0.2	0.2	0.2	0.2
Yb	0.9	0.9	1.0	1.0	1.0	1.2	1.1	1.3	1.2	1.2
Lu	0.1	0.1	0.1	0.1	0.1	0.2	0.2	0.2	0.2	0.2
Element Ratios										
Mg#	58.4	54.8	54.1	52.8	56.1	51.4	48.3	46.9	49.8	20.0
Cr/V	9.7	7.2	6.8	6.2	6.3	3.7	4.0	3.8	3.1	0.9
Eu/Eu*	1.2	0.9	0.9	1.0	1.0	0.9	1.0	0.9	1.0	0.7
Ni/Cu	2.8	2.7	2.5	0.5	0.7	0.9	1.4	0.8	0.5	4.4
Cu/Pd	15250	2900	4583	1928	1841	3095	2667	3632	4251	5000
Pd/Pt	1.0	1.0	1.0	2.7	2.9	2.2	2.3	2.9	3.1	1.3

Eu/Eu* calculated by $Eu_N / (Sm_N * Gd_N)^{0.5}$

Table 2. Chalcophile element concentrations of gabbroic rocks at Idefix.

Sample	Unit	Base Metal (wt.%)		Platinum Group Elements & Gold (ppb)*						S (wt.%)
		Ni	Cu	Ir	Ru	Rh	Pt	Pd	Au	
1D11-02	I1	2.1	5.2	55	69	642	2166	17228	173	2.0
1D11-07D	I1	2.9	8.7	118	88	1086	14650	64878	1036	0.8
1D11-14	I1	2.4	2.3	117	95	859	6361	18375	348	2.3
1D11-04	I3	3.2	14.0	372	211	3119	20354	68939	3578	2.8
1D11-06	I3	3.2	11.3	328	221	2968	22333	74725	2486	0.8
1D11-12	I3	0.4	26.7	331	178	2887	20619	67258	12670	3.2
1D11-13	I3	3.1	19.0	827	477	6794	43641	156154	3205	1.3
1D11-24	I3	0.7	14.1	725	415	6080	2372	76511	1732	1.6
1D11-01	Barren	2.1	8.2	330	194	2969	30544	100081	2008	0.5

*Normalised to 100% sulphide using the method of Barnes & Lightfoot (2005).

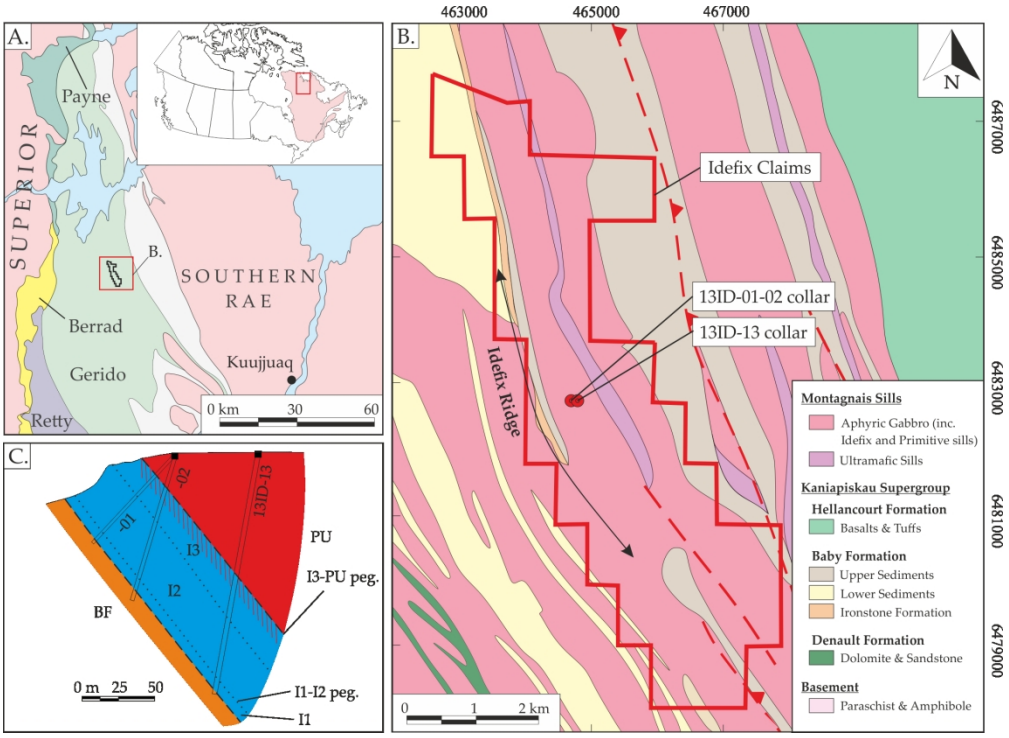

a. Location of the study area in the lithotectonic divisions of Clark and Wares (2005). b. Geological map of the Idefix PGE-Cu prospect, showing the outline of the property and location of the boreholes addressed in this study. c. Cross-section across the centre of the property, showing the intersections of the labelled boreholes.

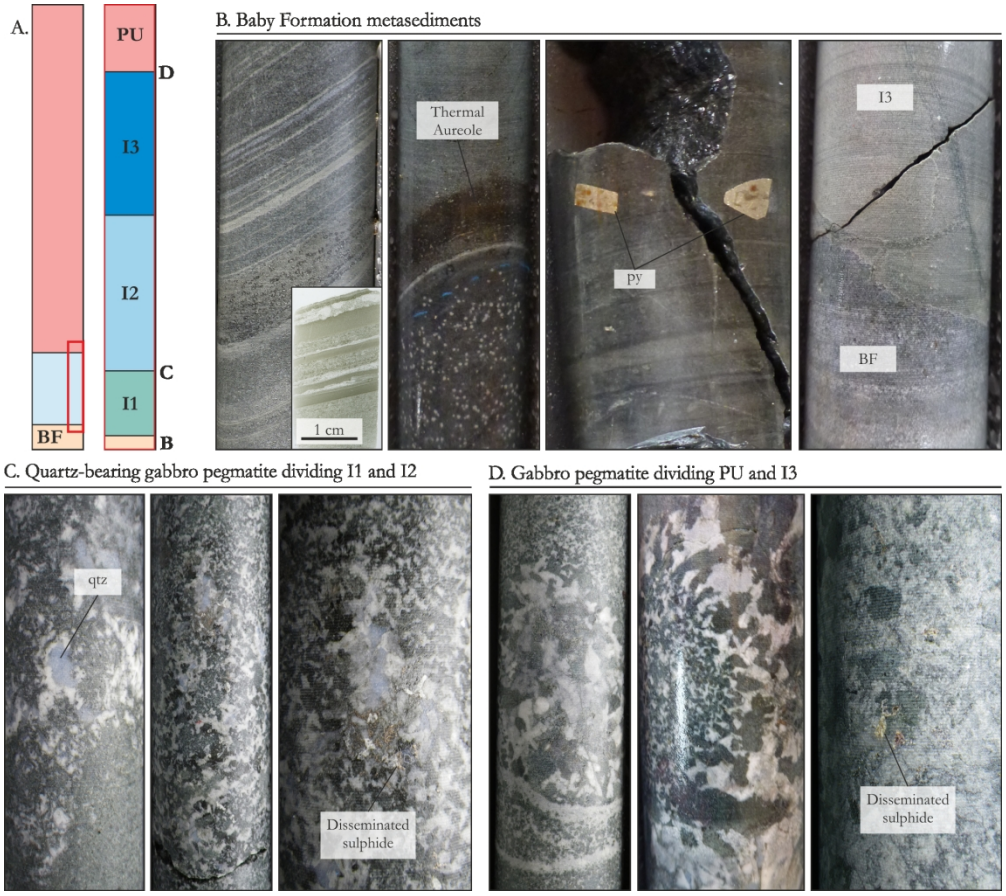

a. Schematic stratigraphy of the Idefix PGE-Cu prospect, showing the divisions of the Idefix sill. b. Textures and characteristics of the Baby Formation metasediments. c. Nature of the gabbroic pegmatite at the I1-I2 contact. d. Nature of the gabbroic pegmatite at the I3-PU contact. rill core is ~ 4 cm in diameter. BF = Baby Formation, py = pyrite, qtz = quartz.

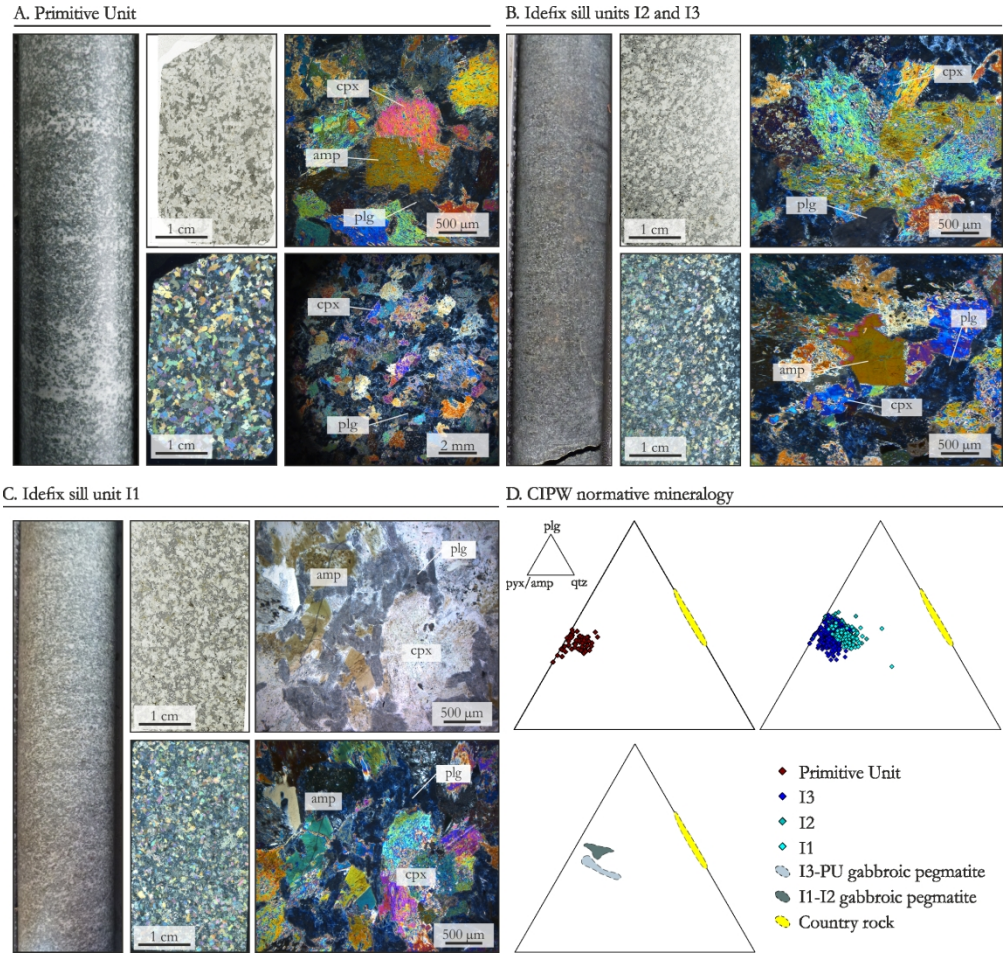

Texture and petrography of (a) the Primitive Unit. (b) Idefix unit I3 and I2, (c) Idefix unit I1. d. CIPW normative mineralogy of gabbroic and gabbroic pegmatitic rocks at Idefix. cpx = clinopyroxene, plg = plagioclase, amp = amphibole, qtz = quartz.

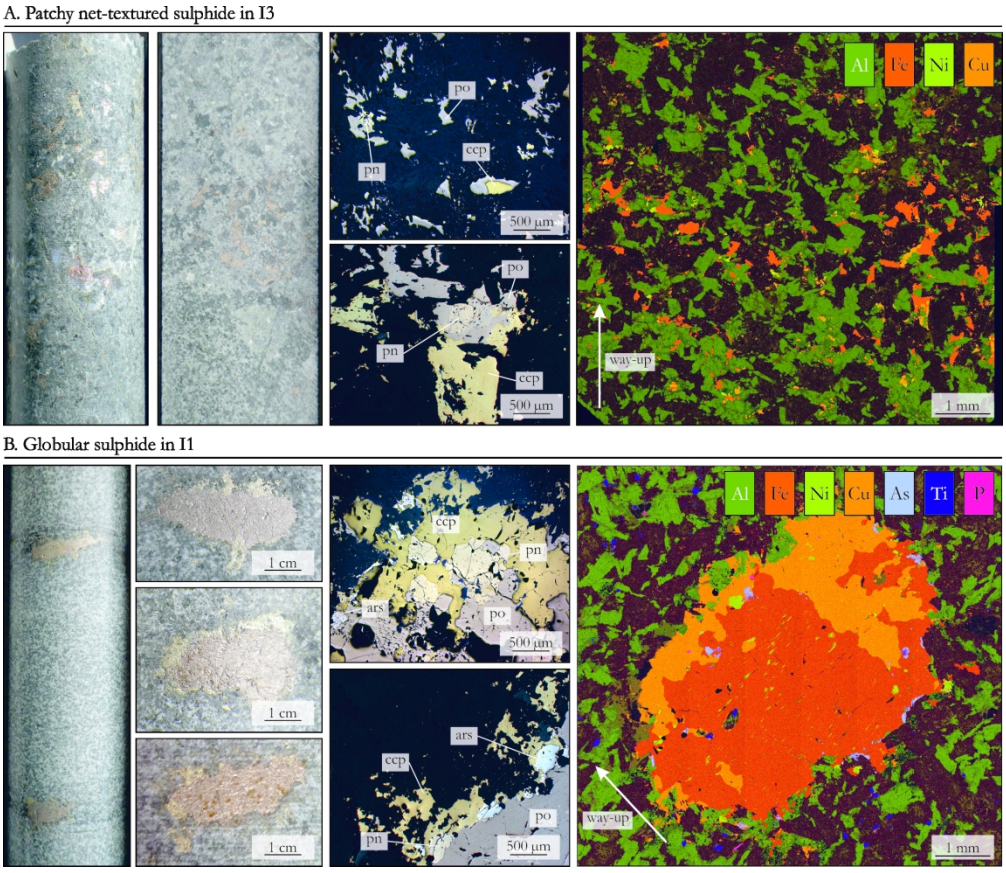

a. Texture and mineralogy of patchy net-textured sulphide. b. Texture and mineralogy of globular sulphide. Note the elliptical shape of the sulphide globules. po = pyrrhotite, pn = pentlandite, ccp = chalcopyrite, ars = sulpharsenides.

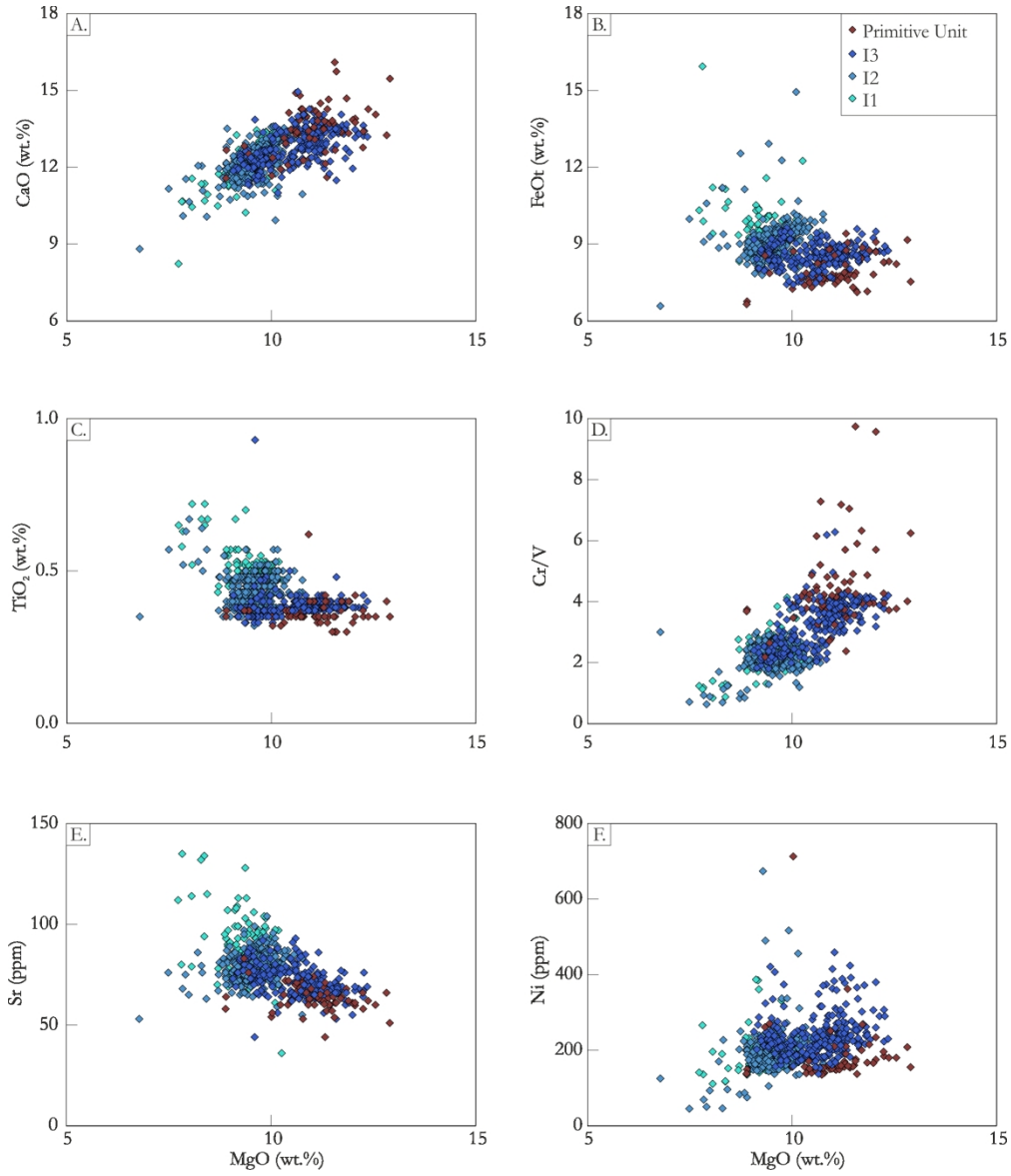

a-f. MgO against CaO, FeOt, TiO2, Cr/V, Sr, and Ni.

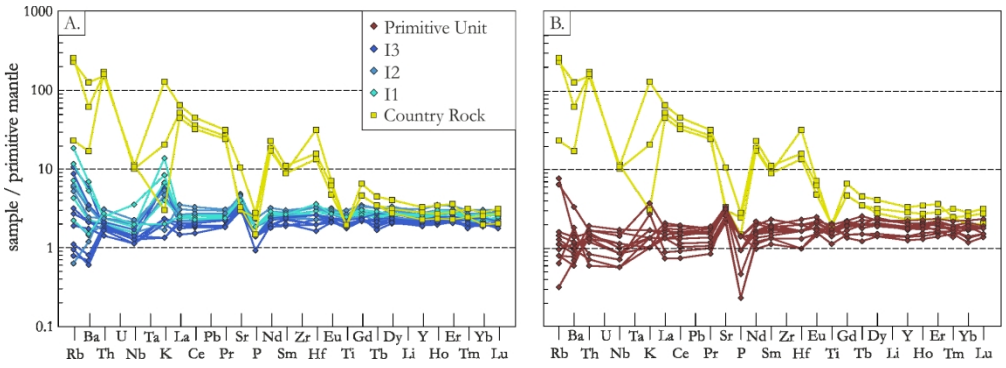

a-b. Primitive mantle normalised (Sun and McDonough 1989) lithophile multi-element plots.

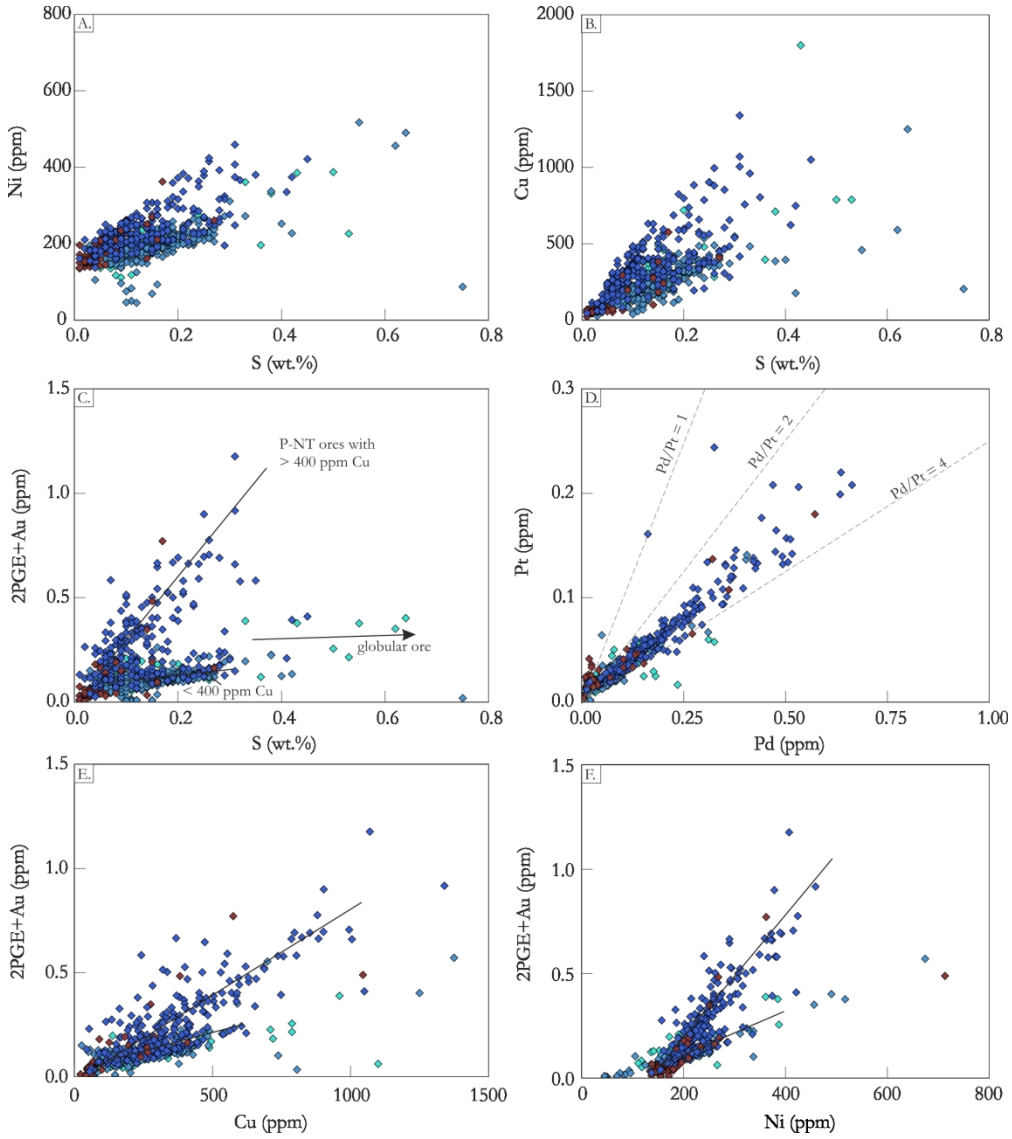

a-c. Sulphur against Ni, Cu, and 2PGE + Au. d. Pd against Pt, whereby net-textured and globular ores correlate at Pt/Pd values of ~ 2.8. e. Cu against 2PGE + Au. f. Ni against 2PGE + Au. Note the different trends in net-textured and globular ores in plots c, e, and f.

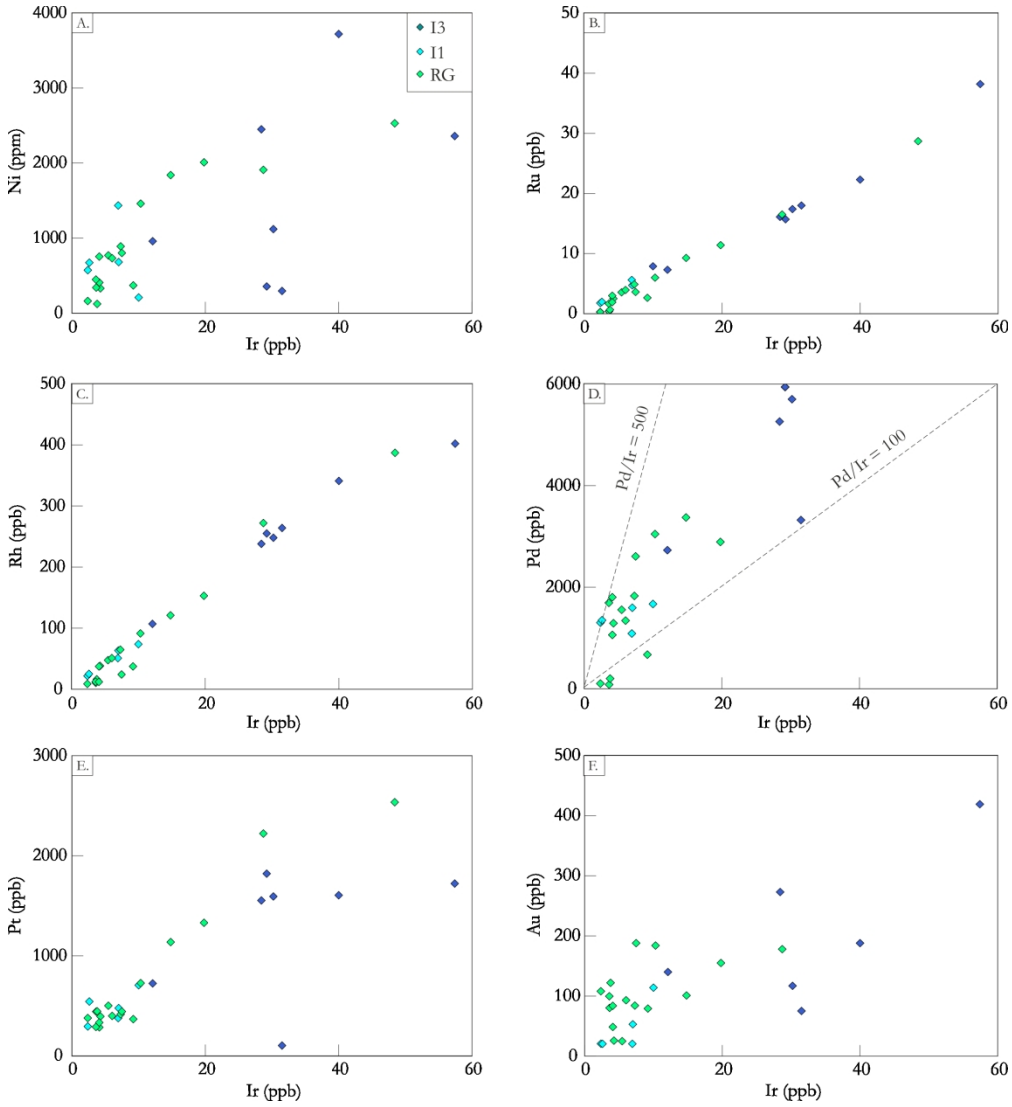

a-f. Ir against Ni, Ru, Rh, Pd, Pt, and Au. Note that IPGE and Pt show good positive correlations (R2 > 0.8) and that all samples plot with Pd/Ir values below 500. RG = regional gabbro.

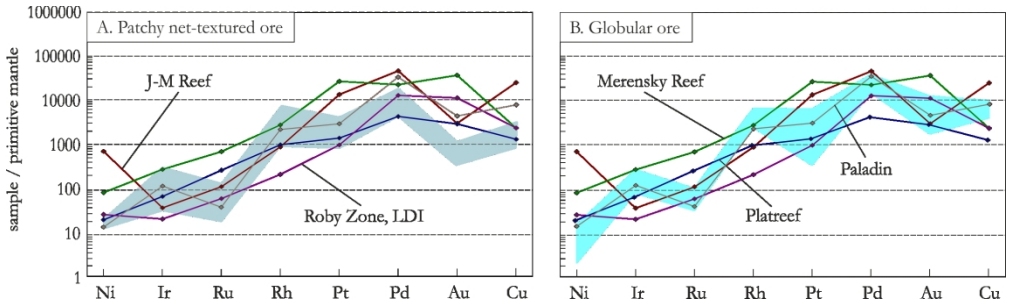

Primitive mantle normalised (Barnes and Maier 1999) chalcophile multi-element plots for (a) patchy net-textured ores and (b) globular ores. For comparison, profiles form the J-M Reef (Godel et al. 2002), Roby Zone of Lac des Iles (LDI; Hinchey et al. 2005), Merensky Reef (Barnes and Maier 2002), the Platreef at Rooipoort (Maier et al. 2008a), and the Paladin deposit in the Labrador Trough (Clark and Wares 2005). All samples with > 0.5 wt.% S have been normalised to 100% sulphide using the method of Barnes and Lightfoot (2005).

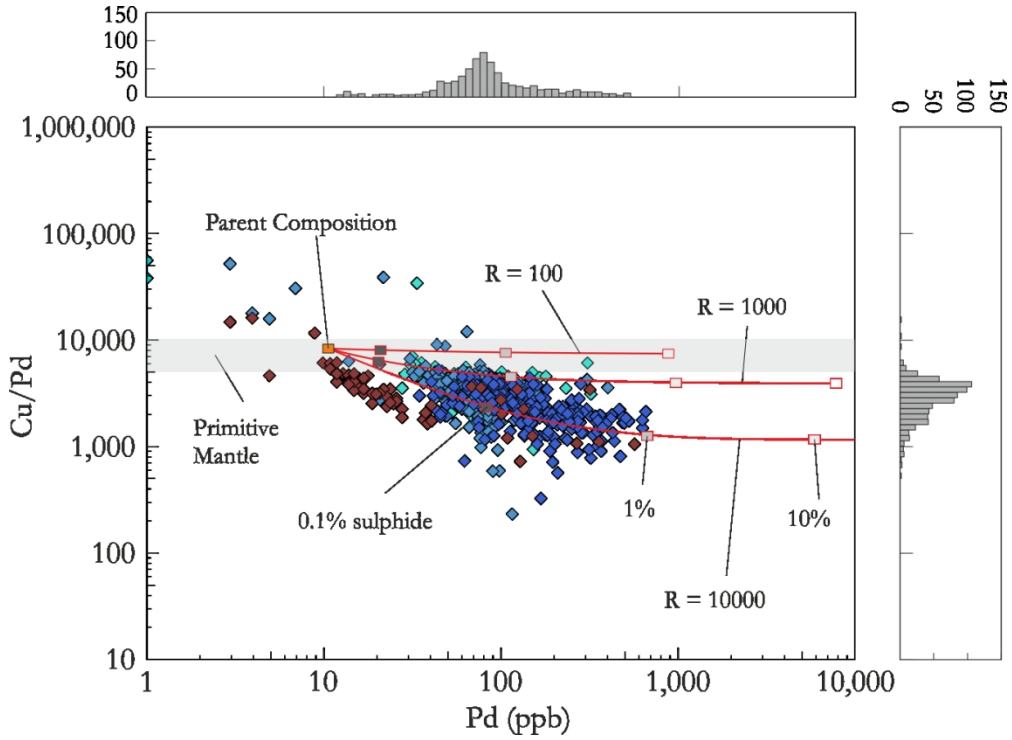

Pd against Cu/Pd with marginal histograms. The underlain grey field represents the expected Cu/Pd range of mantle rock (Barnes and Maier 1999). Grey boxes represent the composition of sulphide at different whole-rock volumes at different R factors (see text for discussion).

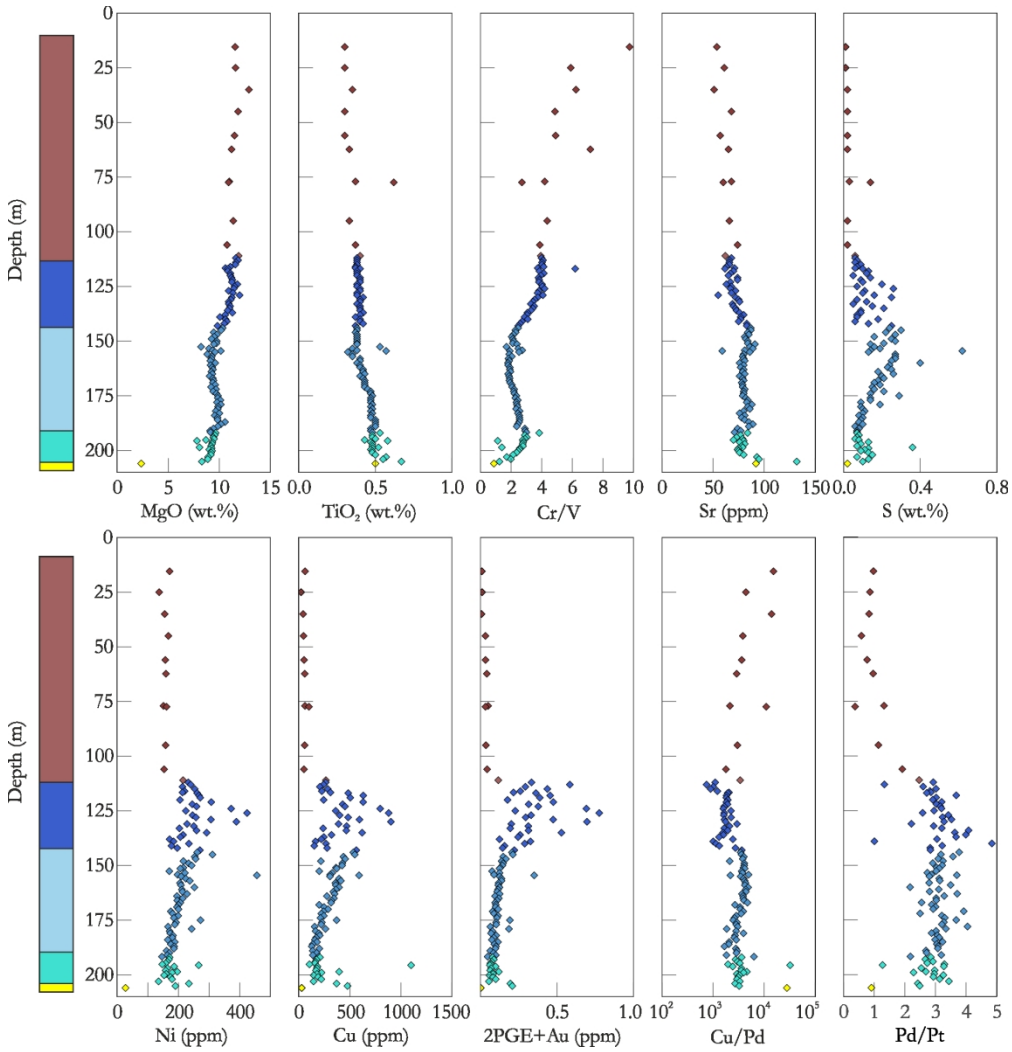

Downhole geochemistry of borehole 13ID-13, showing the downward trend of lithophile and chalcophile elements.

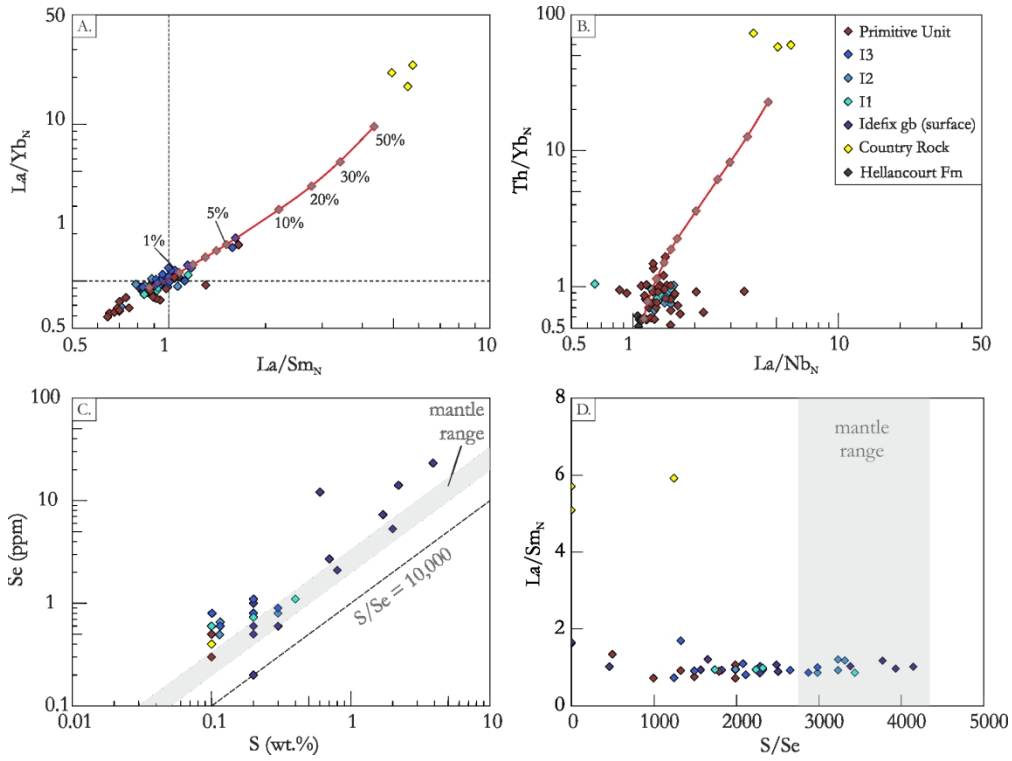

a-b. La/SmN against La/YbN and La/NbN against Th/YbN, overlain with binary mixing models between Hellancourt basalt (Ciborowski et al. 2017) and Baby Formation sediments. c. S against Se underlain with that of mantle range (2850 to 4300; Eckstrand and Hulbert 1987). Note that all samples plot at or just below that expected for mantle rock. d. S/Se against La/SmCN showing no changes in La/SmN values relative to S/Se. Normalised ratios were normalised using values of Sun and McDonough (1989).

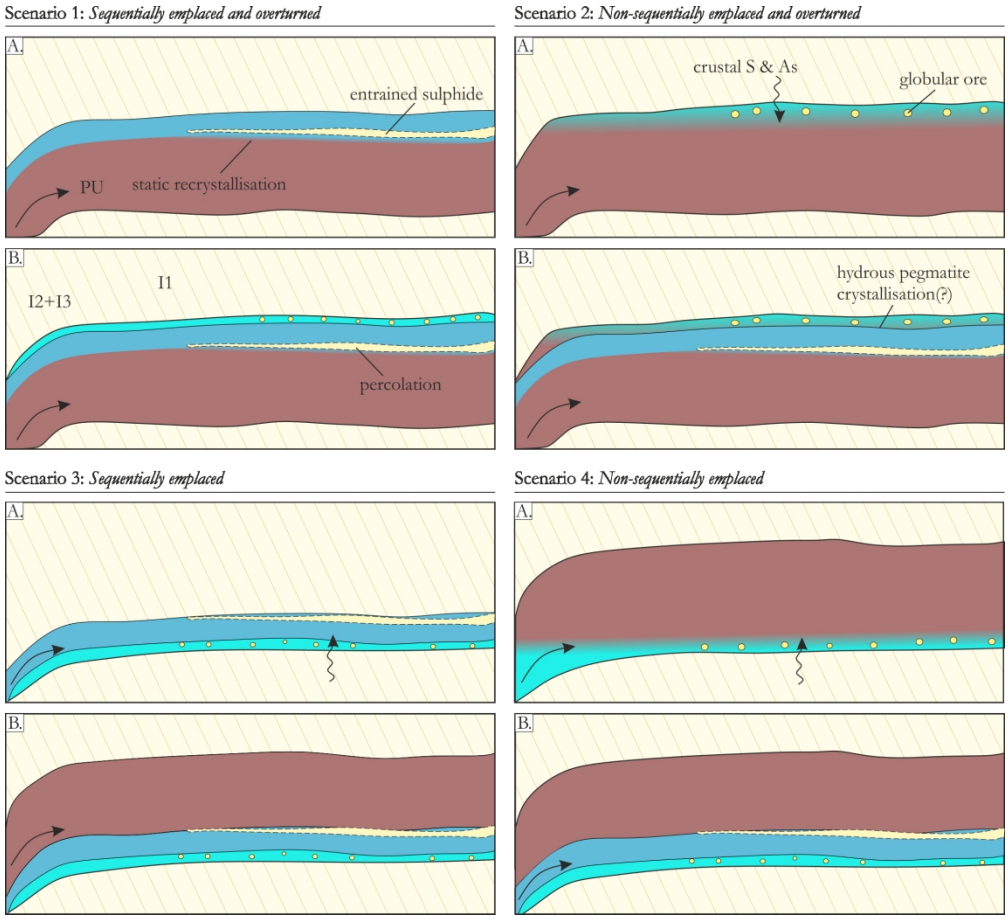

Emplacement scenarios for the gabbroic rocks at Idefix if (1) sequentially emplaced and overturned, (2) non-sequentially emplaced and overturned, (3) sequentially emplaced, and (4) non-sequentially emplaced.